Supporting Information

Luo et al. 10.1073/pnas.1219028109

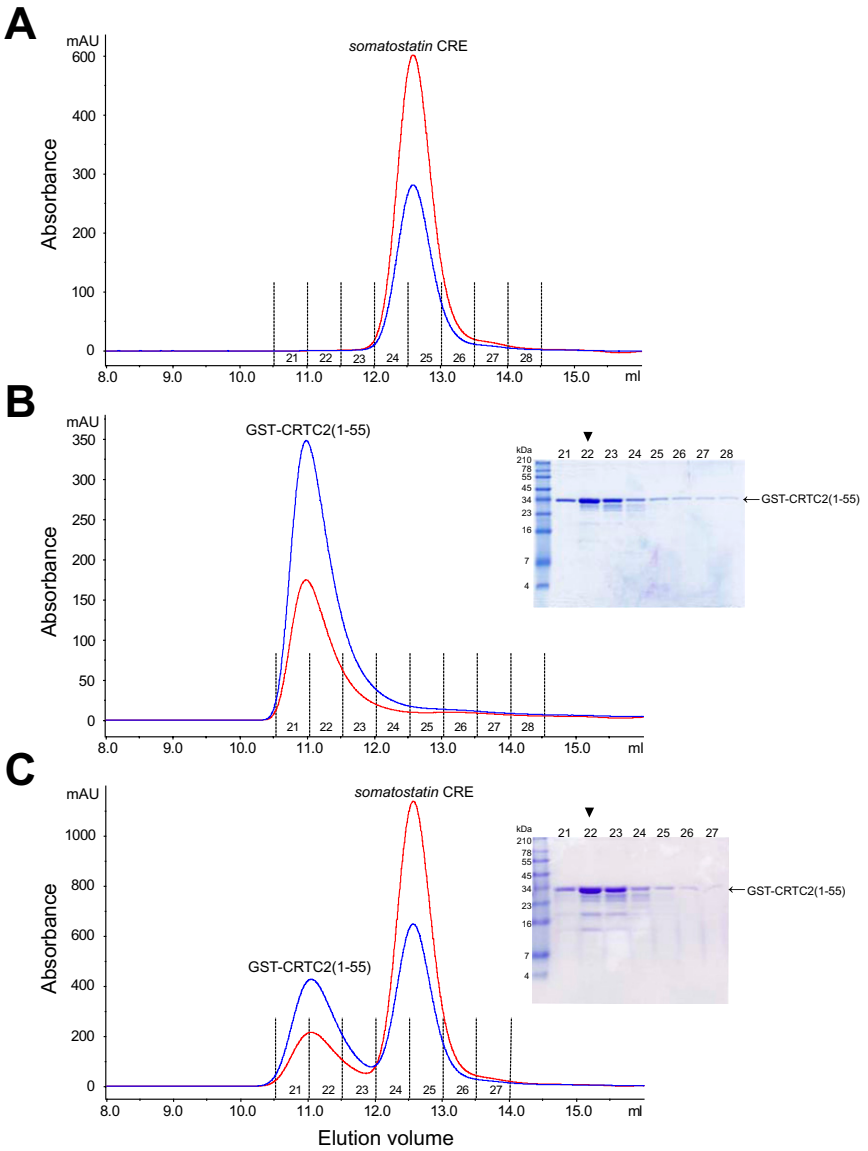

Fig. S1. Size exclusion chromatography (SEC) analyses demonstrate the lack of a direct interaction between cAMP response element binding protein (CREB)-regulated transcriptional coactivator (CRTC) 2 and DNA. Elution profiles of samples of (*A*) free DNA duplex harboring a *somatostatin* cAMP response element (CRE), (*B*) free GST-CRTC2 (1–55), and (*C*) a 2:1 stoichiometric mixture of GST-CRTC2 (1–55) and *somatostatin* CRE. Samples were injected into a Superdex 75 column and eluted with 20 mM Mops buffer (pH 6.5) containing 150 mM NaCl, 5 mM $MgCl_2$, 1 mM EDTA, and 2 mM DTT. UV absorbances at 260 (red) and 280 (blue) nm were monitored. The proteins in each of the eluted fractions were resolved by SDS/PAGE and visualized by Coomassie staining. Note that because of the instrumental setup, there is a consistent ~0.5-mL lag between when a peak is detected by UV (at 260 and 280 nm) and the appearance of the corresponding protein bands in the gel. To guide the reader, selected lanes in the gels have been annotated with arrows on top to identify the location of the peaks in the chromatograms corresponding to the GST-CRTC2 (1–55) protein.

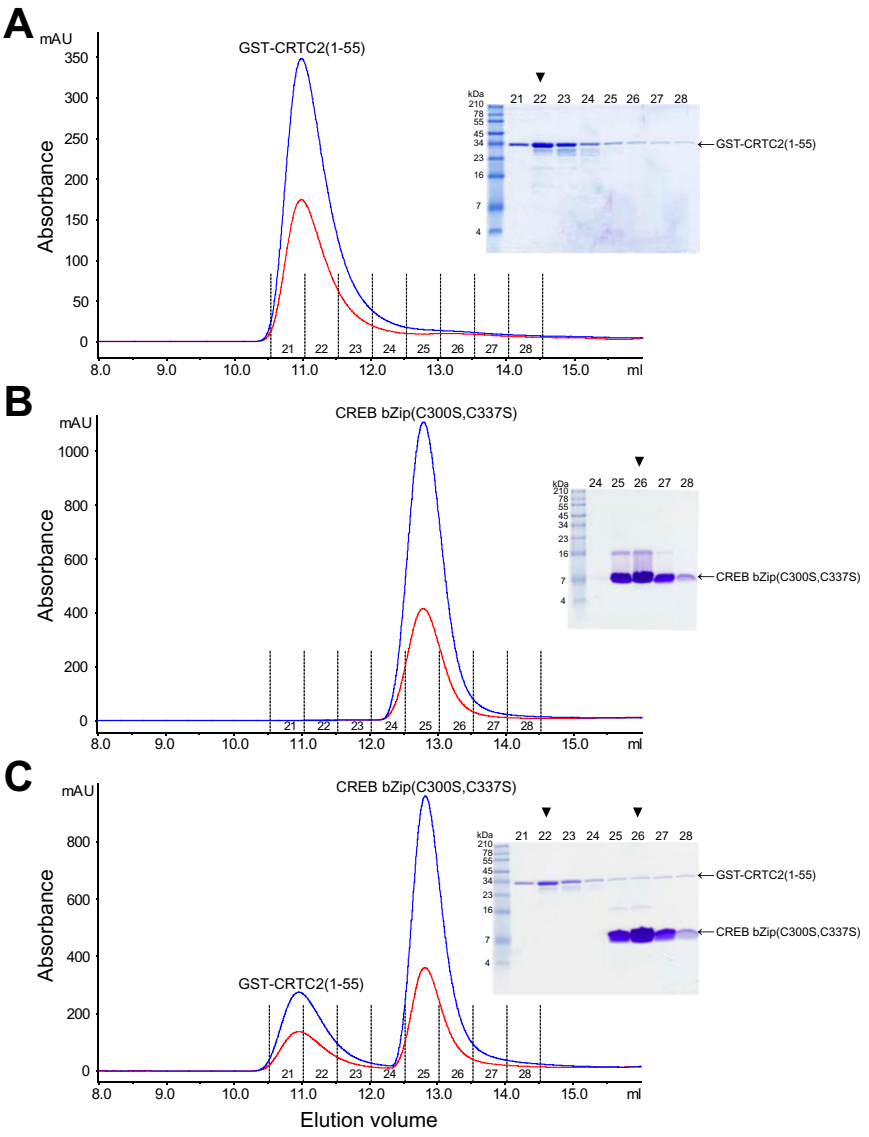

Fig. S2. SEC analyses demonstrate the lack of an interaction between CRTC2 and CREB in the absence of DNA. Elution profiles of samples of (*A*) free GST-CRTC2 (1–55), (*B*) free CREB basic leucine zipper (bZip) C300S,C337S, and (*C*) a 1:10 stoichiometric mixture of GST-CRTC2 (1–55) and CREB bZip C300S,C337S. Samples were injected into a Superdex 75 column and eluted with 20 mM Mops buffer (pH 6.5) containing 150 mM NaCl, 5 mM $MgCl_2$, 1 mM EDTA, and 2 mM DTT. UV absorbances at 260 (red) and 280 (blue) nm were monitored. The proteins in each of the eluted fractions were resolved by SDS/PAGE and visualized by Coomassie staining. Note that because of the instrumental setup, there is a consistent ~0.5-mL lag between when a peak is detected by UV (at 260 and 280 nm) and the appearance of the corresponding protein bands in the gel. To guide the reader, selected lanes in the various gels have been annotated with arrows on top to identify the location of the peaks in the chromatograms corresponding to the GST-CRTC2 (1–55) and CREB bZip C300S,C337S proteins.

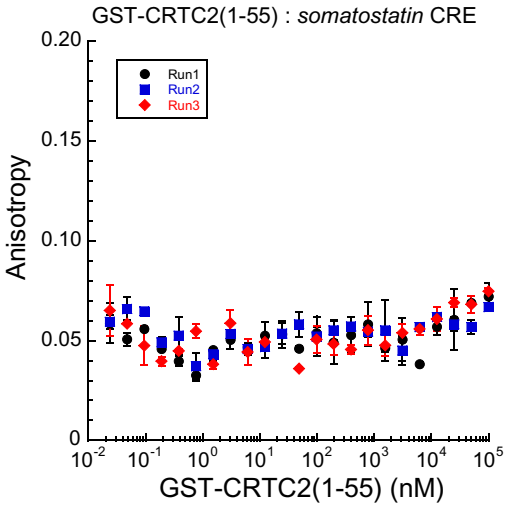

Fig. S3. Fluorescence anisotropy (FA) assays demonstrate the absence of a direct interaction between CRTC2 and DNA. FA curves from titrations conducted with a fluoresceinated double-stranded oligonucleotide harboring a *somatostatin* cAMP response element (CRE) with increasing amounts of GST-CRTC2 (residues 1–55). The results from three independent experiments (different colored symbols) are shown.

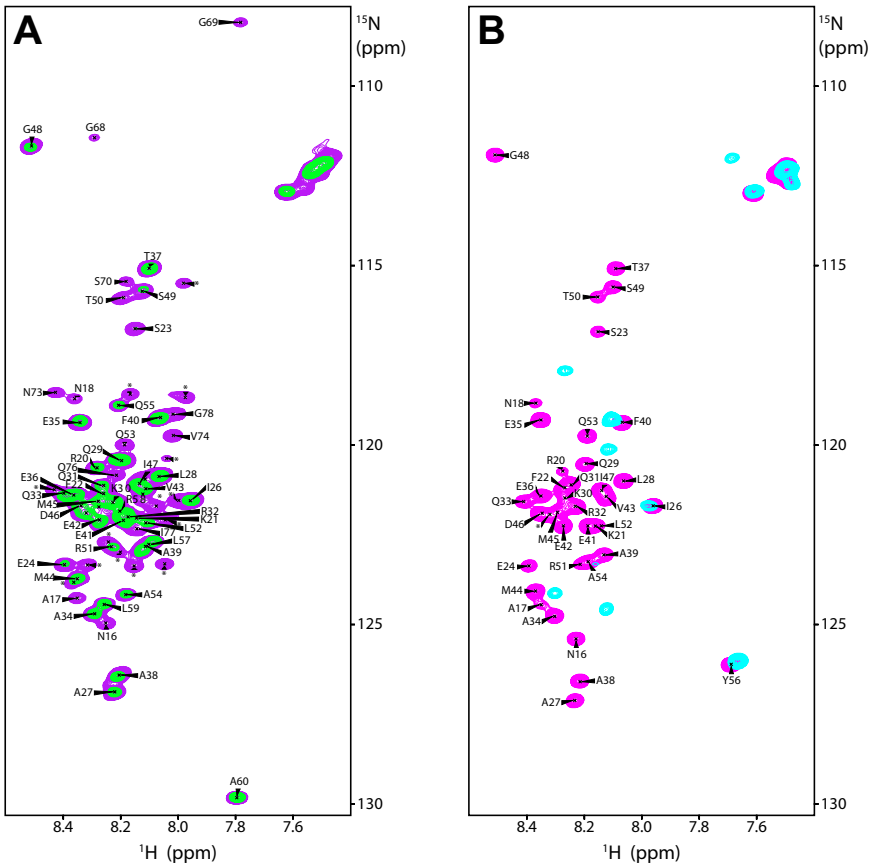

Fig. S4. NMR analyses reveal a largely unstructured conformation for CRTC2 peptides harboring the CREB binding domain (CBD). (*A*) ^{1}H-^{15}N correlated spectra of the apo-CRTC2 (18–78) peptide recorded immediately after sample preparation (purple) and after 90 h (green). The spectra were acquired, processed, and displayed using identical parameters. Assignments are annotated. The spectrum is characterized by poor amide proton chemical shift dispersion and narrow resonances linewidths, characteristic of unstructured peptides. Asterisks denote unassigned resonances, a large subset of which is suspected to arise owing to conformational heterogeneity. All resonances undergo line broadening with time, indicative of aggregation, although a subset of resonances are more severely affected. Time-dependent aggregation precluded detailed studies of the peptide in the context of the ternary complex. (*B*) ^{1}H-^{15}N correlated spectra of the CRTC2 (18–55) peptide in the apo- (magenta) and in the ternary complex with CREB bZip bound to *somatostatin* CRE (cyan). The spectra were acquired and processed using identical parameters. The spectrum of apo-CRTC2 (18–55) bears the same hallmarks of unstructured peptides like apo-CRTC2 (18–78), but unlike apo-CRTC2 (18–78), it shows no evidence of time-dependent aggregation. Note that the resonance positions for most resonances, barring the nonnative tyrosine residue (Y56) at the C terminus, have changed in the ternary complex likely owing to their proximity to the binding interface. Because of the larger size of the ternary complex (32 KDa), the sensitivity of this spectrum is considerably lower and hence is plotted at fivefold lower threshold than the spectrum for the apo-protein.

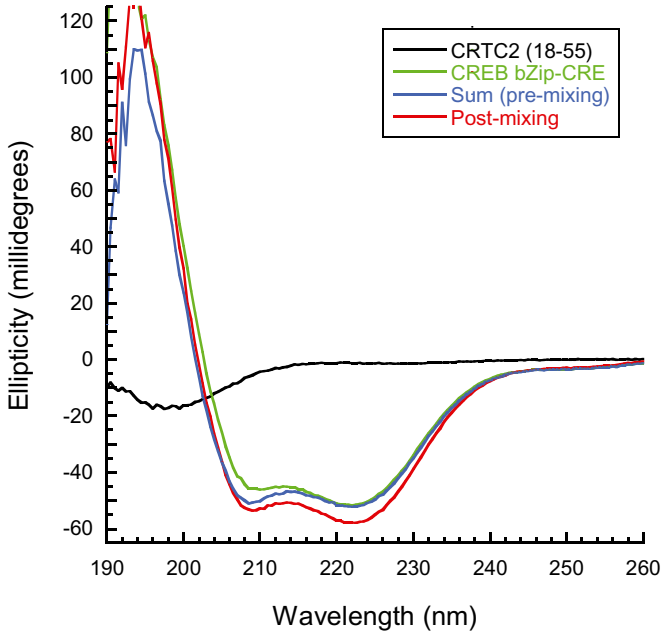

Fig. S5. Circular dichroism spectra reveal enhancement in helical content upon ternary complex formation. CD spectra of apo-CRTC2 (18-55; black) and CREB bZip:CRE complex (green); sum spectra recorded before and after mixing are shown in blue and red, respectively. Sample concentrations were 2.5 μM of double-stranded DNA harboring a *somatostatin* CRE and 5 μM each of CRTC2 (18–55) and CREB bZip. Data presented are averages of three scans. Notice the enhancement in intensity of the bands at 208 and 222 nm, characteristic of helical conformation, upon ternary complex formation relative to apo-CRTC2 CBD and the CREB bZip:CRE binary complex. Because the CREB bZip is already almost completely helical in complex with DNA (Protein Data Bank ID: 1DH3), we attribute the intensity enhancements to the acquisition of stable helical structure (notably absent in the apo-form) for CRTC2 CBD in the ternary complex.

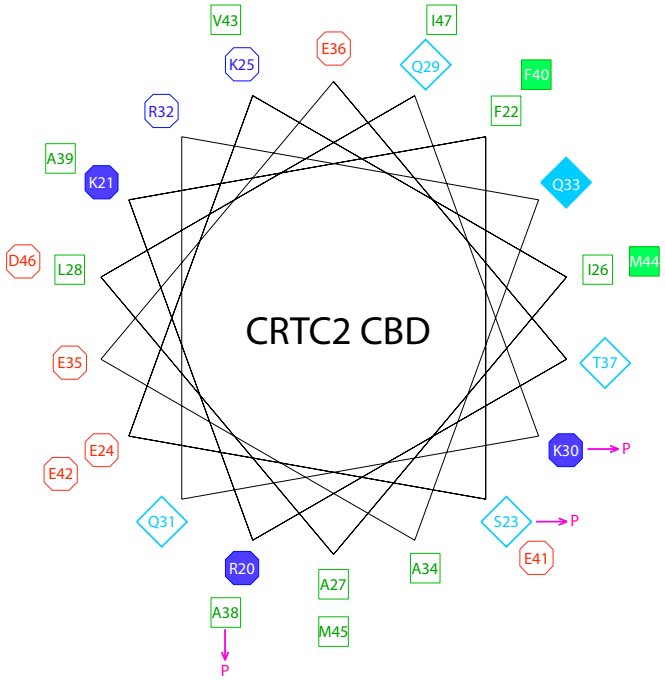

Fig. S6. CRTC2 CBD mutations mapped on to a helical wheel. Residues are colored according to type: polar (cyan), basic (deep blue), acidic (red), and hydrophobic (green). Mutations that strongly perturb CREB binding are indicated by filled boxes; these cluster on one face of the helix. Arrows identify the locations of the proline mutations. Note that Arg20 and Lys21 are located at the N terminus of the CBD helix on the opposite face poised to interact with DNA.

Table S1. Summary of the expected and measured molecular masses of the principal eluting species in SECMALS experiments

Molecular species	Expected mass (kg/mol)	Measured mass (kg/mol)
Half-site CRE (double-stranded)	8.5	8.5 ± 0.2
CREB bZip(C300S,C337S) (monomer)	7.2	—
CREB bZip(C300S,C337S):half-site CRE (2:1)	22.8	20.9 ± 1.4
CRTC2(1-116) (monomer)	15.1	—
CRTC2(1-116):CREBbZip(C300S,C337S):half-site CRE (2:2:1)	53.0	53.7 ± 1.2
CRTC2(18-78) (monomer)	9.4	—
CRTC2(18-78):CREBbZip(C300S,C337S):half-site CRE (2:2:1)	41.5	41.4 ± 1.1
CRTC2(18-70) (monomer)	8.5	—
CRTC2(18-70):CREBbZip(C300S,C337S):half-site CRE (2:2:1)	39.9	36.2 ± 0.5
CRTC2(18-55) (monomer)	4.8	—
CRTC2(18-55):CREBbZip(C300S,C337S):half-site CRE (2:2:1)	32.4	28.1 ± 0.9
GST-CRTC2(1-55) (dimer)	64.6	58.8 ± 2.7
GST-CRTC2(1-55):CREB bZip(C300S,C337S):half-site CRE (2:2:1)	87.4	84.6 ± 1.9

— indicates not determined.

Table S2. Summary of equilibrium binding data from fluorescence anisotropy assays

Reactant 1	Reactant 2	EC_{50} (nM)
CREB bZip	*somatostatin* CRE	11.7 ± 5.4
CREB bZip	Half-site CRE	68.9 ± 5.9
CREB bZip	*G6Pase* CRE	144.8 ± 29.7
CRTC2(1-116)	CREB bZip:*somatostatin* CRE	97.1 ± 43.1*
GST-CRTC2(1-55)	CREB bZip:*somatostatin* CRE	358.0 ± 28.6
GST-CRTC2(1-55)	CREB bZip:half-site CRE	1,104 ± 110
GST-CRTC2(1-55)	CREB bZip:*G6Pase* CRE	498.3 ± 20.5
CREB bZip(C300S)	*somatostatin* CRE	7.1 ± 1.6
CREB bZip(C300S)	Half-site CRE	40.4 ± 5.7
CREB bZip(C300S)	*G6Pase* CRE	66.5 ± 11.4
CREB bZip(C300S,C337S)	*somatostatin* CRE	3.7 ± 1.4
CREB bZip(C300S,C337S)	Half-site CRE	17.5 ± 7.1
CREB bZip(C300S,C337S)	*G6Pase* CRE	26.3 ± 7.2
CREB bZip(C300S,C310S,C337S)	*somatostatin* CRE	3.8 ± 0.6
CREB bZip(C300S,C310S,C337S)	Half-site CRE	17.4 ± 3.6
CREB bZip(C300S,C310S,C337S)	*G6Pase* CRE	30.9 ± 9.9
CRTC2(1-116)	CREB bZip(C300S):*somatostatin* CRE	23.3 ± 2.8
CRTC2(1-116)	CREB bZip(C300S,C337S):*somatostatin* CRE	23.4 ± 3.3
GST-CRTC2(1-55)	CREB bZip(C300S):*somatostatin* CRE	22.4 ± 6.4
GST-CRTC2(1-55)	CREB bZip(C300S):half-site CRE	232.6 ± 36.4
GST-CRTC2(1-55)	CREB bZip(C300S):*G6Pase* CRE	223.9 ± 34.2
GST-CRTC2(1-55)	CREB bZip(C300S,C337S):*somatostatin* CRE	16.0 ± 5.1
GST-CRTC2(1-55)	CREB bZip(C300S,C337S):half-site CRE	190.0 ± 16.0
GST-CRTC2(1-55)	CREB bZip(C300S,C337S):*G6Pase* CRE	183.4 ± 21.6
GST-CRTC2(1-55)	CREB bZip(C300S,C310S,C337S):*somatostatin* CRE	3,817 ± 738
GST-CRTC2(1-55)	CREB bZip(C300S,C310S,C337S):half-site CRE	54,665 ± 4,560
GST-CRTC2(1-55)	CREB bZip(C300S,C310S,C337S):*G6Pase* CRE	44,744 ± 1,834
GST-CRTC2(1-55) K30A	CREB bZip(C300S,C337S):*somatostatin* CRE	190 ± 26†
GST-CRTC2(1-55) Q33A	CREB bZip(C300S,C337S):*somatostatin* CRE	114 ± 23†
GST-CRTC2(1-55) T37A	CREB bZip(C300S,C337S):*somatostatin* CRE	36 ± 2†
GST-CRTC2(1-55) F40A	CREB bZip(C300S,C337S):*somatostatin* CRE	>121,000†
GST-CRTC2(1-55) M44A	CREB bZip(C300S,C337S):*somatostatin* CRE	>355,000†
GST-CRTC2(1-55) S23P	CREB bZip(C300S,C337S):*somatostatin* CRE	8,162 ± 1,039†
GST-CRTC2(1-55) K30P	CREB bZip(C300S,C337S):*somatostatin* CRE	8,906 ± 2,232†
GST-CRTC2(1-55) A38P	CREB bZip(C300S,C337S):*somatostatin* CRE	NDB
GST-CRTC2(1-55) R20E,K21E	CREB bZip(C300S,C337S):*somatostatin* CRE	579.8 ± 56.6†
CREB bZip(C300S,C337S,Y307A)	*somatostatin* CRE	502 ± 92†
CREB bZip(C300S,C337S,R314A)	*somatostatin* CRE	171 ± 18†
CREB bZip(C300S,C337S,Q321A)	*somatostatin* CRE	12.4 ± 0.4†
GST-CRTC2(1-55)	CREB bZip(C300S,C337S,Y307A):*somatostatin* CRE	>30,000†
GST-CRTC2(1-55)	CREB bZip(C300S,C337S,R314A):*somatostatin* CRE	2,544 ± 89†
GST-CRTC2(1-55)	CREB bZip(C300S,C337S,Q321A):*somatostatin* CRE	1,464 ± 98†

All measurements done with $n = 6$, except: *$n = 10$, and †$n = 3$; NDB, no detectable binding.

Table S3. Crystallographic structure determination and refinement statistics for CRTC2 (18–50)

Variable	SeMet CRTC2(18-50)
Data collection	
Resolution range (Å)	15–1.80 (1.83–1.80)
Space group	C 2
Unit cell (Å, °)	a = 21.5, b = 57.6, c = 23.1 $\alpha = \gamma = 90$, $\beta = 94.6$
Observations	
Unique	2,595
Total	19,070
Redundancy	7.3 (7.4)
Completeness (%)	99.4 (100)
$I/\sigma(I)$	22 (14.9)
R_{sym}*	0.087 (0.134)
Phasing	
Phasing power†	2.2
$R_{Cullius}$†	0.56
Figure of merit	0.51
Refinement	
Resolution range (Å)	14.41–2.0
No. of reflections	1,817
R-factor‡	0.25 (0.33)
R_{free}§	0.28 (0.33)
Monomers/asymmetric unit	1
No. of atoms	
Protein, nonhydrogen	231
Nonprotein	30
rmsd	
Length (Å)	0.004
Angle (°)	0.707
Overall B-factor (Å)	13.1

Values in parentheses are for the highest-resolution shell.

*$R_{sym} = \Sigma|I_{obs} - I_{avg}|/\Sigma I_{obs}$ where the summation is over all reflections.

†From autoSHARP for acentric reflections.

‡*R*-factor = $\Sigma|F_o\text{-}F_c|/\Sigma F_o$.

§For calculation of R_{free}, 4.3% of the reflections were reserved.